Stem Cell Reports
Article

OPEN ACCESS

Direct Genesis of Functional Rodent and Human Schwann Cells from Skin Mesenchymal Precursors

Matthew P. Krause,[1,2,9] Shaalee Dworski,[1,3,9] Konstantin Feinberg,[1,2,9] Karen Jones,[1,2,9] Adam P.W. Johnston,[1,2] Smitha Paul,[1,2] Maryline Paris,[2,8] Elior Peles,[7] Darius Bagli,[2,5,6] Christopher R. Forrest,[2,6] David R. Kaplan,[1,3,4] and Freda D. Miller[1,2,3,4,5,*]

[1]Program in Neuroscience and Mental Health
[2]Program in Developmental and Stem Cell Biology
Hospital for Sick Children, Toronto, ON M5G 1L7, Canada
[3]Institute of Medical Science
[4]Department of Molecular Genetics
[5]Department of Physiology
[6]Department of Surgery
University of Toronto, Toronto, ON M5G 0A4, Canada
[7]Department of Molecular Cell Biology, Weizmann Institute of Science, Rehovot 7632700, Israel
[8]Present address: L'Oreal Research and Innovation 1, Avenue Eugène Schueller, Aulnay-sous-Bois 93600, France
[9]These authors contributed equally to this work
*Correspondence: fredam@sickkids.ca
http://dx.doi.org/10.1016/j.stemcr.2014.05.011

SUMMARY

Recent reports of directed reprogramming have raised questions about the stability of cell lineages. Here, we have addressed this issue, focusing upon skin-derived precursors (SKPs), a dermally derived precursor cell. We show by lineage tracing that murine SKPs from dorsal skin originate from mesenchymal and not neural crest-derived cells. These mesenchymally derived SKPs can, without genetic manipulation, generate functional Schwann cells, a neural crest cell type, and are highly similar at the transcriptional level to Schwann cells isolated from the peripheral nerve. This is not a mouse-specific phenomenon, since human SKPs that are highly similar at the transcriptome level can be made from neural crest-derived facial and mesodermally derived foreskin dermis and the foreskin SKPs can make myelinating Schwann cells. Thus, nonneural crest-derived mesenchymal precursors can differentiate into bona fide peripheral glia in the absence of genetic manipulation, suggesting that developmentally defined lineage boundaries are more flexible than widely thought.

INTRODUCTION

The skin is a highly regenerative organ containing distinct populations of adult precursors that serve to maintain this regenerative capacity. One of these is a SOX2-positive dermal precursor that resides in hair follicles and that can regenerate the dermis and induce hair follicle morphogenesis (Biernaskie et al., 2009; Fernandes et al., 2004). When these cells (termed skin-derived precursors, or SKPs) are expanded in culture, they differentiate into mesenchymal cell types like smooth muscle cells, adipocytes, and dermal fibroblasts (Biernaskie et al., 2009; Lavoie et al., 2009; Steinbach et al., 2011; Toma et al., 2001, 2005) and peripheral neural cells such as Schwann cells (Biernaskie et al., 2007; Hunt et al., 2008; McKenzie et al., 2006). This differentiation repertoire is reminiscent of embryonic neural crest precursors and, consistent with this, SKPs exhibit many neural crest precursor-like properties (Fernandes et al., 2004). However, lineage tracing recently showed that SKPs isolated from facial skin come from the neural crest, while SKPs from dorsal skin derive instead from a somite origin (Jinno et al., 2010), as does the rest of the dorsal dermis (Mauger, 1972). In spite of these different origins, dorsal and facial SKPs are very similar at the transcriptome level (Jinno et al., 2010).

These findings indicate that cells of different developmental origins can converge to generate somatic tissue precursor cells with highly similar phenotypes. However, they also raise a number of important questions. In particular, while it is generally thought that only the neural crest generates peripheral neural cells like Schwann cells, these findings suggest that mesenchymal precursors of nonneural crest origin might have the same capacity. Support for this idea comes from studies showing that functional Schwann cells can be generated from mesenchymal precursors (for example, see McKenzie et al., 2006; Caddick et al., 2006) and that genetic manipulation can reprogram dermal cells directly into functional neural progeny (reviewed in Abdullah et al., 2012). However, these findings are complicated by the fact that neural crest precursors are present in peripheral nerves and thus potentially in mesenchymal cell preparations from skin or other innervated tissues. For example, we showed that SKPs from dorsal dermis generated Schwann cells (McKenzie et al., 2006; Biernaskie et al., 2007), but others suggested these were of neural crest origin (Wong et al., 2006). Thus, a key question

is whether these neural progeny derive from mesenchymal precursors or from widespread neural crest precursors.

Here, we have used lineage tracing to address this issue and show that nonneural crest dermal mesenchymal cells can generate myelinating Schwann cells that are highly similar to nerve-derived Schwann cells. This is not a mouse-specific phenomenon, since highly similar SKPs can be made from neonatal human foreskin and facial dermis, tissues thought to be mesodermally versus neural crest derived, respectively. In addition, the human foreskin SKPs make myelinating Schwann cells. Thus, nonneural crest-derived mesenchymal precursors can differentiate into bona fide peripheral glia in the absence of genetic manipulation, indicating that developmentally defined lineage boundaries are more flexible than widely thought.

RESULTS

Dorsal Rodent SKPs Derive from Dermal Mesenchymal Cells

We previously showed that rodent facial SKPs come from the neural crest, whereas SKPs from the dorsal dermis derive from *Myf5-Cre*-positive cells, a marker for a somite origin (Jinno et al., 2010). To definitively ask whether dorsal SKPs come from dermal mesenchymal cells, we used mice with Cre recombinase knocked in to the *Dermo1* locus (*Dermo1*$^{Cre/+}$ mice; Yu et al., 2003). Dermo1 is a basic helix-loop-helix that is expressed in embryonic dermal cells and some other mesenchymal cell types (Li et al., 1995). We crossed the *Dermo1*$^{Cre/+}$ mice to mice with a floxed YFP gene in the *Rosa26* locus to cause Cre-dependent expression of YFP in dermal mesenchymal precursors and their progeny. Immunostaining of dorsal skin from *Dermo1*$^{Cre/+}$;*R26YFP*$^{fl/+}$ mice showed that virtually all dermal cells were YFP positive, including those thought to give rise to SKPs, the neural cell adhesion molecule (NCAM)-positive cells in the hair follicle dermal papilla and smooth muscle actin (SMA)-positive cells in the dermal sheath (Figures 1A–1C). In contrast, neural crest-derived cells, including tyrosinase-positive melanocytes and S100β-positive Schwann cells in skin nerves, were YFP negative (Figures 1D and 1E).

To confirm that Schwann cells were negative for the reporter, we examined the sciatic nerve of *Dermo1*$^{Cre/+}$;*R26TdTomato*$^{fl/+}$ mice. TdTomato-positive cells were present in the nerve epineurium and perineurium, with the occasional positive cell in nerve fascicles, likely endoneurial fibroblasts. None of these cells colocalized with the Schwann cell marker S100β (Figures 1F and 1G), although they were positive for fibronectin and CD34 (Figures 1H and 1I). Thus, dorsal mesenchymal and not neural crest cells are labeled in these mice.

We therefore cultured SKPs from neonatal dorsal dermis of *Dermo1*$^{Cre/+}$;*R26YFP*$^{fl/+}$ mice to ask whether they came from mesenchymal cells. Almost all spheres were positive for YFP (Figure 2A) as well as SOX2 (Figure 2B), nestin, and fibronectin (Figure 2C), well-characterized SKP markers. Similar results were obtained following passaging (Figures 2E–2H). Sectioning of spheres from *Dermo1*$^{Cre/+}$;*R26TdTomato*$^{fl/+}$ mice (Figure 2D) showed that virtually all cells were positive for the TdTomato reporter. To address the possibility that *Dermo1-cre* might be turned on by the culture conditions, we sorted YFP-positive and negative cells from *Dermo1*$^{Cre/+}$;*R26YFP*$^{fl/+}$ dorsal skin (Figure 2I) and cultured them under SKP conditions. Only YFP-positive cells made spheres (Figure 2J), as we previously observed with *Myf5-cre*-positive dorsal dermal cells (Jinno et al., 2010). Thus, dorsal SKPs originate from dermal mesenchymal cells that are somite, and not neural crest, derived.

SKPs Generated from Dermal Mesenchymal Cells Differentiate into Functional Schwann Cells

We next asked whether mesenchymally derived SKPs could differentiate into Schwann cells. To obtain pure populations of reporter gene-positive SKPs, we made spheres from dorsal skin of neonatal *Dermo1*$^{Cre/+}$;*R26YFP*$^{fl/+}$ or *Dermo1*$^{Cre/+}$;*R26TdTomato*$^{fl/+}$ mice (as shown in Figures 2A–2H), dissociated the spheres, and sorted cells for YFP or TdTomato (Figure 2K). Consistent with the sectioning data (Figure 2D), almost all sphere cells were reporter gene positive (Figure 2K). We then plated the sorted YFP-positive SKP cells under conditions that promote differentiation and survival of Schwann cells (Biernaskie et al., 2006). After 1–2 weeks, we observed patches of YFP-positive cells with a bipolar Schwann cell morphology that could be decorated with a NECL1-Fc (Figure 2L) that binds to NECL4 on live Schwann cells (Maurel et al., 2007). We then used cloning cylinders to isolate the putative SKP-derived Schwann cells (SKP-SCs), replated them, and expanded them under Schwann cell culture conditions (Figure 2M). These cultures were highly enriched for reporter gene-positive, S100β-positive, NECL1-Fc-positive putative Schwann cells (Figures 2M and 2N).

We performed two assays to ask whether these were functional Schwann cells. First, we cultured dorsal *Dermo1*$^{Cre/+}$;*R26TdTomato*$^{fl/+}$ SKP-SCs with axons of neonatal sympathetic neurons in compartmented cultures (Singh and Miller, 2005). Over 8 days, many TdTomato-positive bipolar SKP-SCs associated tightly with axons (Figure 3A), as is seen with primary Schwann cells. We also observed a second subpopulation of TdTomato-positive cells with a flattened morphology (Figure 3A) that did not associate with axons and were presumably SKP-derived

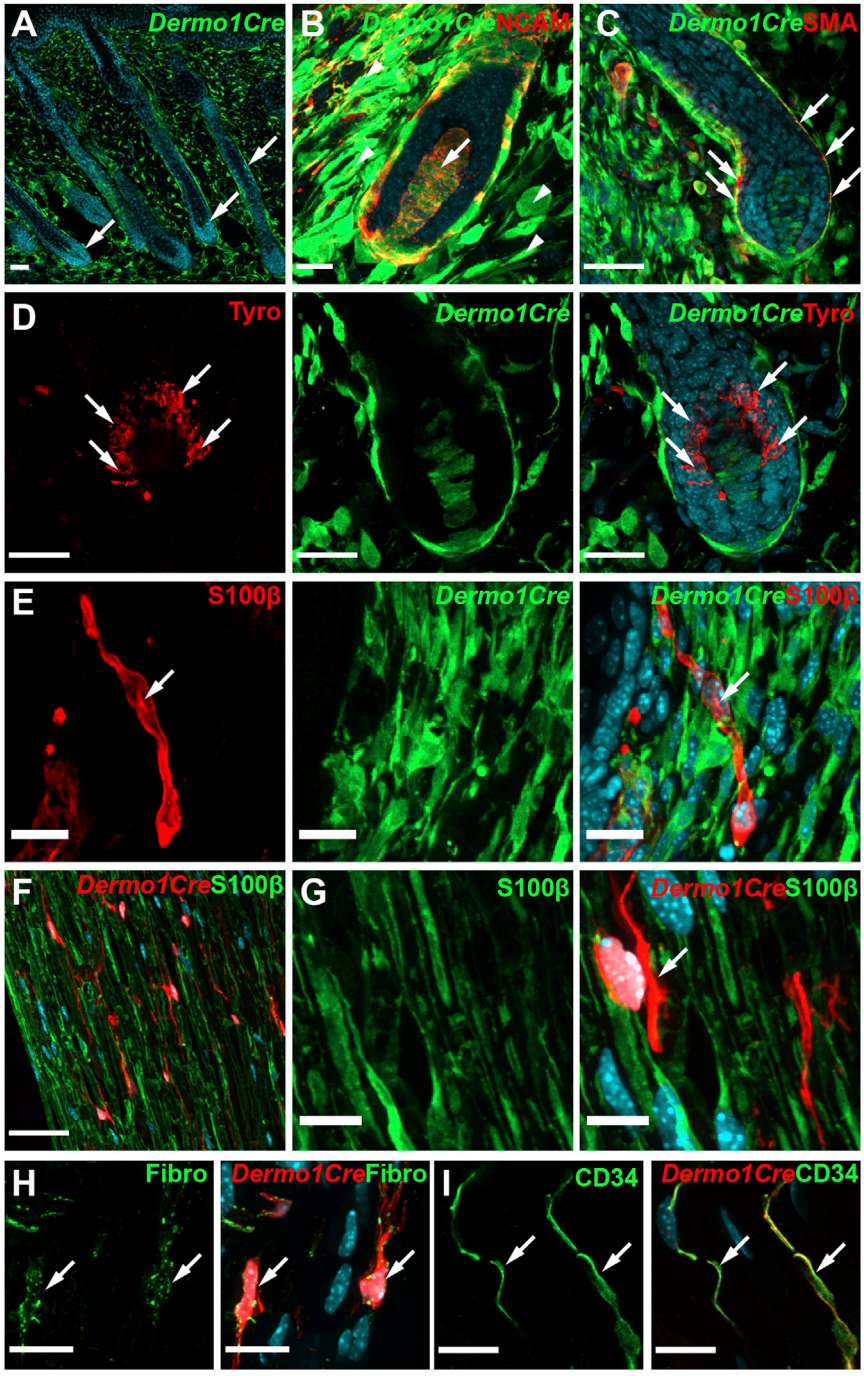

Figure 1. *Dermo1*$^{Cre/+}$-Based Lineage Tracing Shows that Dorsal SKPs Are of Mesenchymal Origin

(A–E) Dorsal backskin sections from adult *Dermo1*$^{Cre/+}$*; R26YFP*$^{fl/+}$ mice were immunostained for YFP (*Dermo1Cre*) and cell-type-specific markers.

(A) Low-magnification micrograph of hair follicles (arrows).

(B and C) Anagen hair follicles immunostained for YFP (green) and NCAM (B) or SMA (C; red in both). Arrow in (B) denotes double-positive cells in the follicle dermal papilla and arrowheads YFP-positive cells in interfollicular dermis. Arrows in (C) denote double-positive follicle dermal sheath cells.

(D) Anagen hair follicle immunostained for YFP (green) and the melanocyte marker tyrosinase (red; right panel shows the merge). Arrows denote tyrosinase-positive melanocytes that are negative for YFP.

(E) Interfollicular dermis immunostained for YFP (green) and the Schwann cell marker S100β (red; the right panel shows the merge). Arrows indicate an S100β-positive, YFP-negative skin nerve.

(F–I) Longitudinal sections of the adult *Dermo1*$^{Cre/+}$*; R26TdTomato*$^{fl/+}$ sciatic nerve immunostained for TdTomato (*Dermo1Cre*; red) and S100β (F and G), fibronectin (H), or CD34 (I; green in all cases). The image in (F) is at low magnification, while (G)–(I) are at high magnification. Arrow in (G) denotes a TdTomato-positive cell that is negative for S100β, while arrows in (H) and (I) show double-positive cells.

In (A)–(I), sections were counterstained with Hoechst 33258 (blue) to highlight nuclei. Scale bars represent 100 μm (A), 25 μm (B, D, and G), 50 μm (C and F), and 15 μm (E, H, and I).

myofibroblasts or dermal fibroblasts (Biernaskie et al., 2009; Steinbach et al., 2011) that were present in the enriched SKP-SC cultures.

Second, we transplanted dorsal *Dermo1*$^{Cre/+}$*;R26YFP*$^{fl/+}$ SKP-SCs into the distal sciatic nerve of adult nonobese diabetic/severe combined immunodeficiency (NOD/SCID) mice immediately following a nerve crush lesion. Thirty days posttransplantation, we immunostained cross sections through the transplanted nerves for YFP to identify the transplanted cells, βIII-tubulin to identify endogenous axons, and myelin-associated glycoprotein (MAG) to identify myelin profiles. This analysis (Figure 3B) identified YFP-positive, MAG-positive cells wrapping endogenous axons, indicating that mesenchymally derived SKP-SCs were functional and capable of myelinating in vivo.

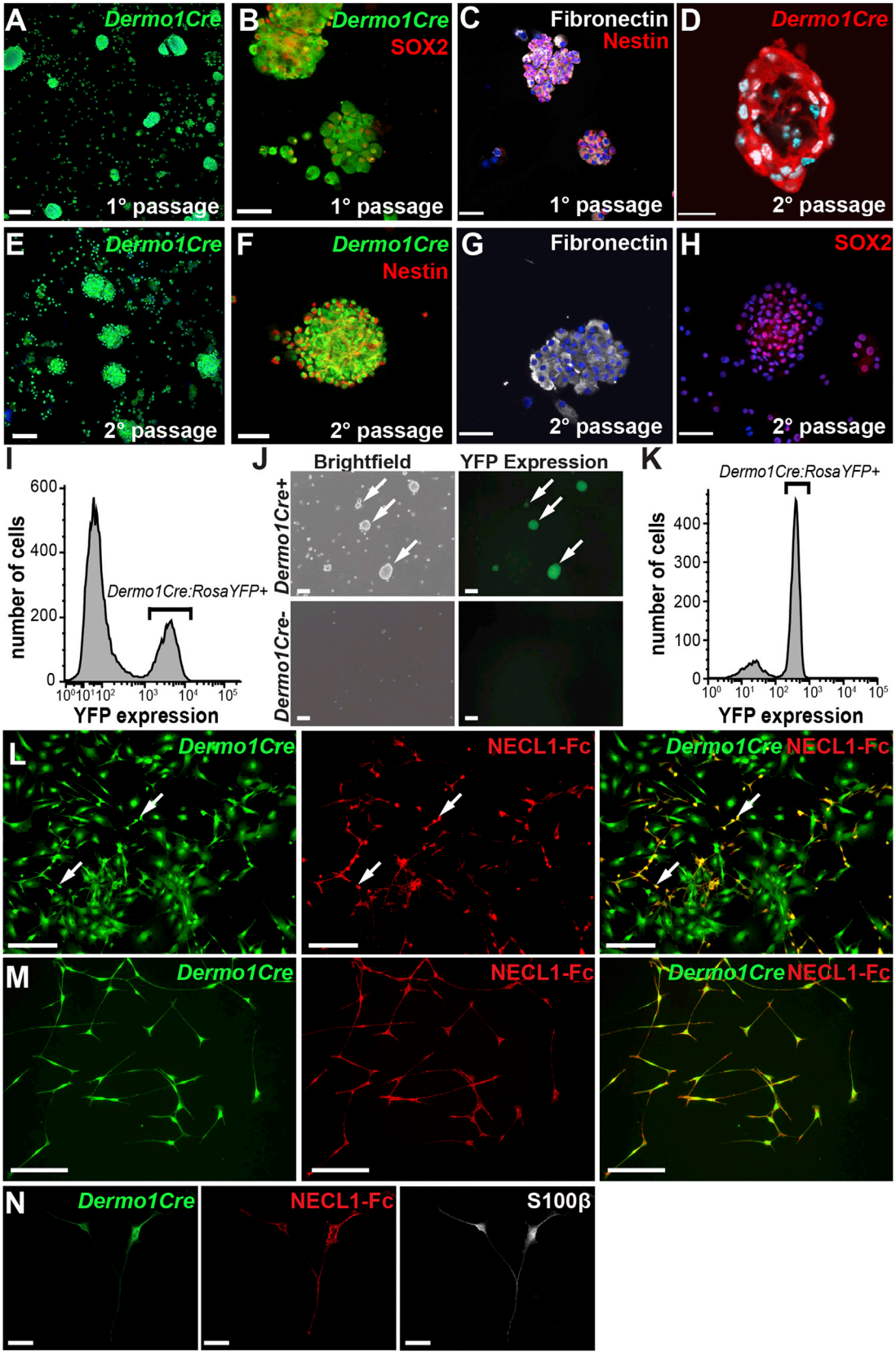

(legend on next page)

Transcriptome Analysis Shows that Mesenchymally Derived SKP-SCs Are Highly Similar to Neural Crest-Derived Nerve Schwann Cells

These data argue that dorsal mesenchymally derived SKPs generate functional Schwann cells in culture. To confirm that these were Schwann cells, we performed microarray analysis to compare them to neural crest-derived Schwann cells from the sciatic nerve. To do this, we made dorsal SKP spheres from adult rats, passaged them three times, dissociated the spheres to single cells, and differentiated them under Schwann cell conditions (Biernaskie et al., 2007, 2006; McKenzie et al., 2006). After 2–3 weeks, we identified Schwann cell colonies visually, isolated them with cloning cylinders, and expanded them in culture. Virtually all of these SKP-SCs were immunopositive for GFAP, S100β, P0, p75NTR, and NECL4 (Figures 3C and 3E). For comparison, we isolated rat sciatic nerve Schwann cells (nerve-SCs) and expanded them as for the SKP-SCs. Immunostaining for the same Schwann cell markers confirmed that these cultures were almost completely pure (Figures 3D and 3E).

We then used microarrays to compare the mesenchymally derived SKP-SCs to the neural crest-derived nerve-SCs, analyzing three biological replicates each with the Affymetrix GeneChip Rat Gene 1.0 ST Array (Gene Expression Omnibus [GEO] accession number GSE57519). We also compared these data to our previously published (Jinno et al., 2010) microarray data from passage 2 adult rat dorsal trunk SKPs. Spearman rank correlation (Figure 4A) showed that SKP-SCs and nerve-SCs were highly similar to each other and were both distinct from undifferentiated SKPs. Unbiased hierarchical clustering using correlation distance and Ward's clustering method confirmed that the SKP-SC and nerve-SC groups were highly similar but distinct from undifferentiated SKPs (Figure 4B) with high confidence (approximately unbiased [AU] p value and bootstrap probability [BP] values between 95 and 100). Nonetheless, the SKP-SC and nerve-SC groups clustered independently, indicating reproducible but minor differences between the two.

To further investigate these similarities and differences, differential expression analysis was performed using the LIMMA bioconductor package (Smyth, 2004; Wettenhall and Smyth, 2004). This analysis demonstrated that only 331 genes showed significant differences of 2-fold or greater between the SKP-SCs and nerve-SCs, while 3,511 were different between SKP-SCs and undifferentiated SKPs ($p < 0.05$, BH) (Figure 4C). Moreover, less than 2% of genes were significantly different between the two Schwann cell populations, while 17% were significantly different between SKP-SCs and undifferentiated SKPs (Figure 4D).

As a further comparison, we analyzed expression of 48 genes that are associated with different stages of Schwann cell differentiation (Figure 4E) (Jessen and Mirsky, 2005). A heatmap of the microarray data showed that SKP-SCs and nerve-SCs were very similar with regard to these Schwann cell genes and that both were distinct from SKPs. RT-PCR for a subset of these—*P0*, *Krox20*, *Sox10*, and *Oct6* mRNAs (Figure 4F)—confirmed that they were approximately similar in the SKP-SC and nerve-SC populations.

We previously showed that mesodermally derived dorsal SKPs and neural crest-derived facial SKPs differentially expressed genes diagnostic of their embryonic origin (Jinno et al., 2010). We asked whether dorsal SKP-SCs retained this memory by performing RT-PCR for two of the dorsal SKPs genes: *Hoxa5* and *Hoxc6* (Figure 4G). While *Hoxa5* mRNA was not detectable in either facial or dorsally derived SKP-SCs, *Hoxc6* mRNA was still expressed in dorsal SKP-SCs (Figure 4G), indicating that they retain some memory of their mesodermal origin.

Figure 2. SKPs Generate Schwann Cells that Can Be Traced to the Dermal Mesenchymal Lineage

(A–C) Primary-passage SKPs generated from the dorsal skin of postnatal day 2 *Dermo1$^{Cre/+}$; R26YFP$^{fl/+}$* mice, immunostained for YFP (A and B, green) and Sox2 (B, red) or fibronectin (C, white) and nestin (C, red).

(D) Confocal micrograph of a section through a secondary-passage SKP sphere generated from an adult *Dermo1$^{Cre/+}$; R26TdTomato$^{fl/+}$* mouse.

(E–H) Secondary-passage SKP spheres generated from *Dermo1$^{Cre/+}$; R26YFP$^{fl/+}$* mice immunostained for YFP (E and F, green) and nestin (F, red), fibronectin (G, white), or SOX2 (H, red).

(I and J) Dorsal skin cells from P2 *Dermo1$^{Cre/+}$; R26YFP$^{fl/+}$* mice were sorted for YFP expression, as shown in the flow cytometry plot in (I), and the YFP-positive (*Dermo1Cre^{+}*) versus YFP-negative (*Dermo1Cre^{-}*) cells were cultured as SKPs for 10 days. Bright-field and fluorescence micrographs (J) show that the YFP-positive cells (green) make SKP spheres (arrows in the top two panels in J), while the YFP-negative cells do not (bottom two panels in J).

(K) Flow cytometry plot of dorsal SKPs generated from P2 *Dermo1$^{Cre/+}$; R26YFP$^{fl/+}$* mice, dissociated and sorted for YFP expression.

(L) YFP-positive SKP cells (green) were sorted as in (K), differentiated under Schwann cell conditions for 14 days, and decorated with NECL1-Fc (red). Arrows denote double-positive cells.

(M and N) SKP-SCs generated as in (K) and (L), isolated, expanded, and immunostained for YFP (M and N, green) and S100β (N, white) and decorated with the NECL1-Fc (M and N, red).

Scale bars represent 200 μm (A, E, and L), 50 μm (B, C, F–H, and N), 25 μm (D), and 100 μm (J and M).

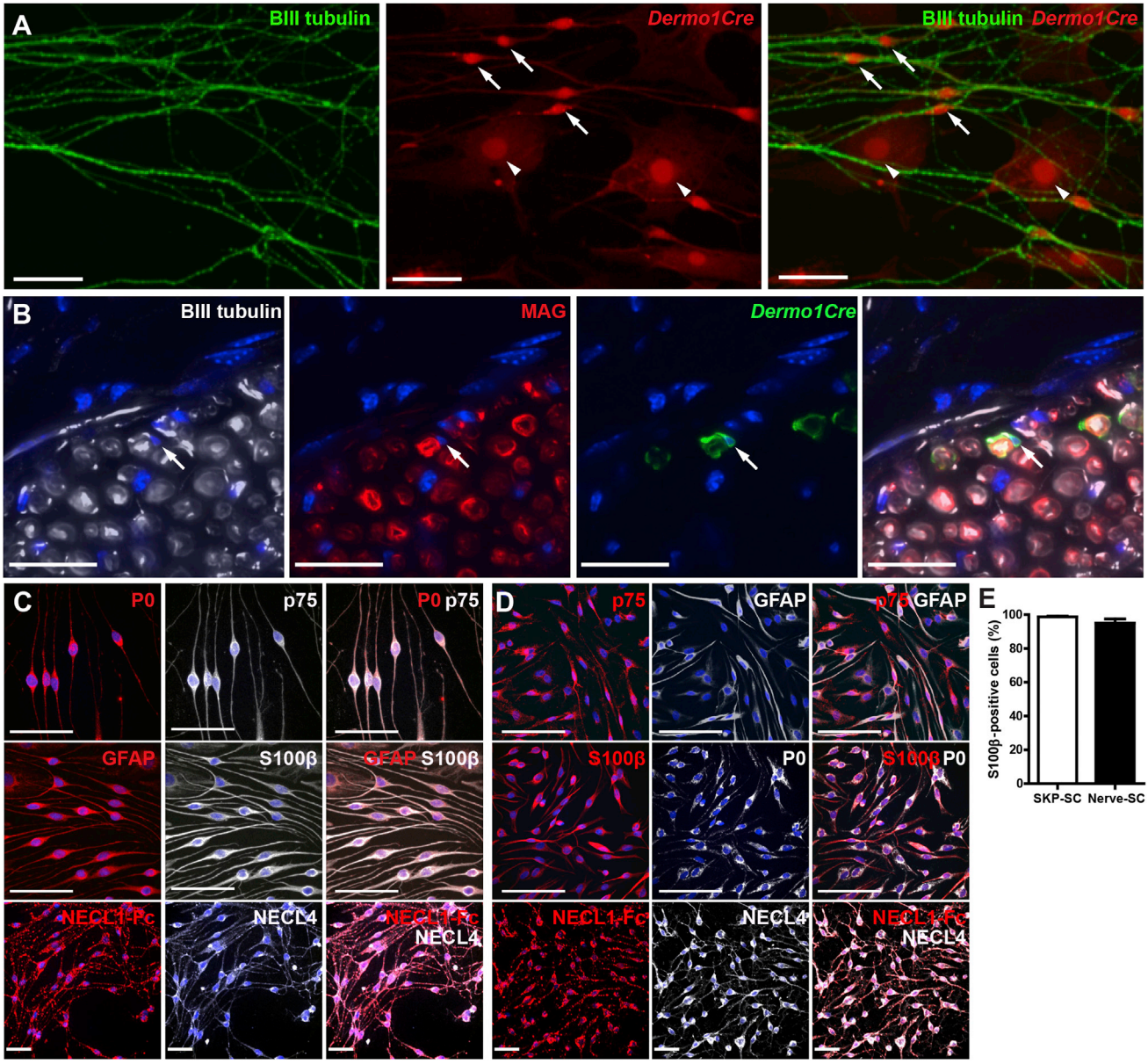

Figure 3. SKP-SCs Exhibit Functional and Phenotypic Similarities to Nerve-SCs

(A and B) Dorsal SKPs from P2 *Dermo1*$^{Cre/+}$*; R26TdTomato*$^{fl/+}$ or *Dermo1*$^{Cre/+}$*; R26YFP*$^{fl/+}$ mice were sorted for reporter gene expression, plated in Schwann cell conditions, and the putative SKP-SCs were enriched using cloning cylinders and expanded. (A) *Dermo1*$^{Cre/+}$*; R26TdTomato*$^{fl/+}$ SKP-SCs cocultured in compartments with sympathetic axons and immunostained 8 days later for TdTomato (red) and the axonal marker βIII-tubulin (green; right panel shows the merge). Arrows and arrowheads denote TdTomato-positive cells that are or are not associated with axons, respectively. (B) Confocal micrographs of a sciatic nerve crushed and transplanted 30 days previously with *Dermo1*$^{Cre/+}$*; R26YFP*$^{fl/+}$ SKP-SCs and immunostained for YFP (green) to detect mesenchymally derived SKP-SCs, βIII-tubulin to show axons (white), and myelin-associated glycoprotein (MAG) (red; the right panel shows the merge) to detect myelin profiles. Section was counterstained with Hoechst (blue). Arrow denotes a YFP-positive cell that has generated a MAG-positive myelin sheath around an axon. (C and D) Micrographs of purified, expanded Schwann cells made from tertiary-passage dorsal SKPs (C) or from adult sciatic nerve (D) that were used for the microarray analysis. Cells were immunostained for various combinations of the Schwann cell markers P0, p75NTR, GFAP, and S100β or were decorated with NECL1-Fc and immunostained for NECL4.

(E) The proportion of S100β-positive cells was determined in immunostained Schwann cell cultures as shown in (C) and (D). n = 3 different preparations each.

Error bars denote the SEM. Scale bars represent 50 μm (A) and 25 μm (B–D).

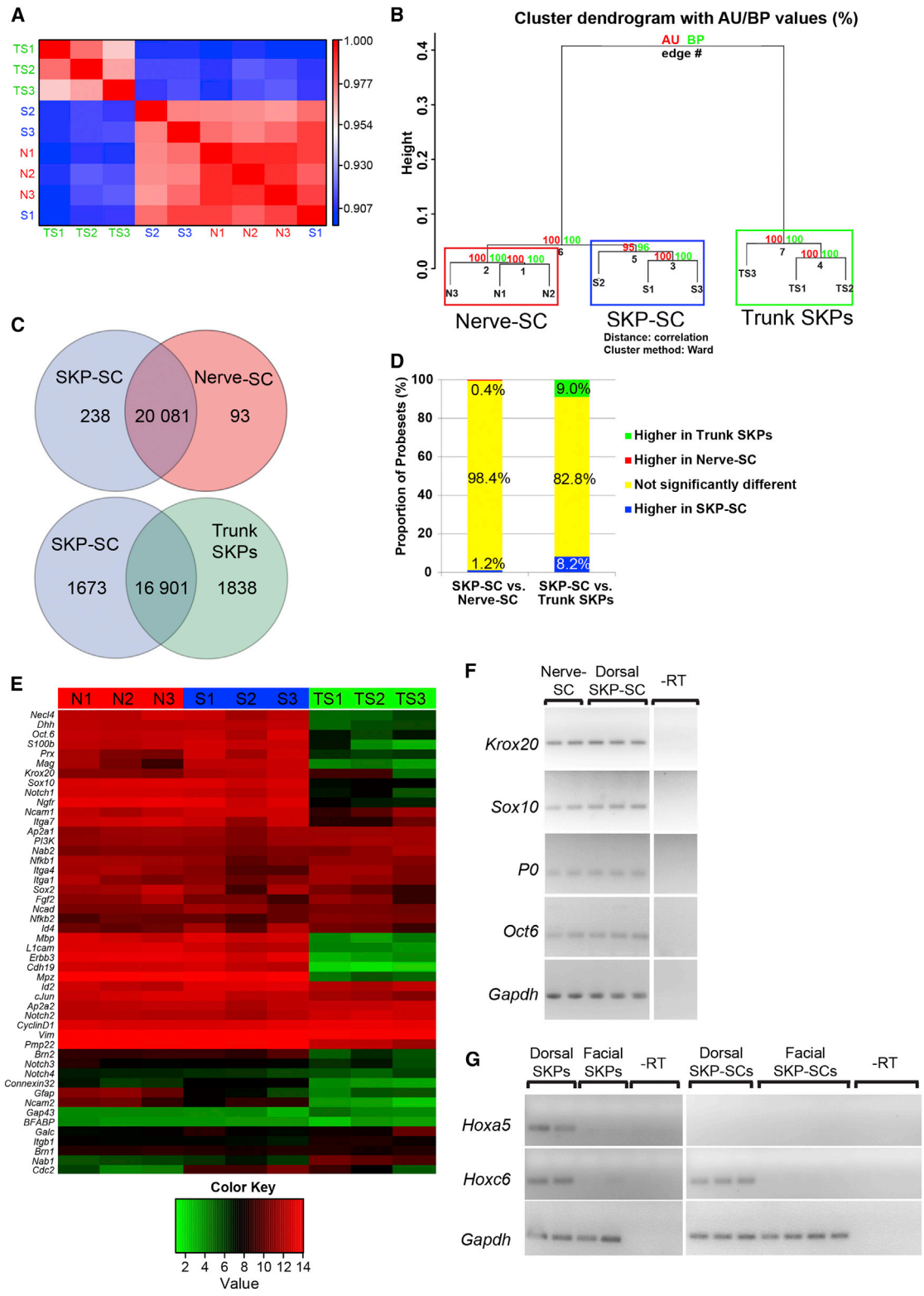

Figure 4. Dorsal SKP-SCs Are Highly Similar to Nerve-SCs but Are Distinct from Dorsal SKPs

Microarray analysis (GEO accession number GSE57519) of three independent isolates each of dorsal adult rat SKP-SCs (SKP-SC 1-3 or S1-3) or adult rat sciatic nerve-SCs (Nerve-SC 1-3 or N1-3), both passaged twice as Schwann cells, and adult rat dorsal trunk SKPs (Trunk SKPs 1-3 or TS1-3).

(legend continued on next page)

Endogenous Dermo1-Positive Mesenchymal Cells Do Not Make Schwann Cells following Injury In Vivo

To ask whether mesenchymal SKPs ever made Schwann cells in vivo as they did in culture, we performed injury experiments. First, we performed full-thickness skin punch wounds, which transect skin nerves that regenerate over the ensuing few weeks. We performed these injuries on *Dermo1$^{Cre/+}$;R26TdTomato$^{fl/+}$* mice that also carried a *Sox2:EGFP* reporter gene, since this labels Schwann cell precursors following skin injury (Johnston et al., 2013). Nine days postinjury, when the skin was healed, we immunostained sections for enhanced GFP (EGFP) to detect the *Sox2* reporter and S100β or p75NTR, which label Schwann cells and their precursors within skin (Johnston et al., 2013). TdTomato expression was also visualized to detect the *Dermo1Cre* reporter. This analysis (Figures 5A and 5B) showed that TdTomato-positive cells within regenerated skin were never positive for EGFP, S100β, or p75NTR.

We also performed nerve injury experiments. The sciatic nerve of adult *Dermo1$^{Cre/+}$;R26TdTomato$^{fl/+}$* mice was crushed and longitudinal nerve sections were immunostained 2 weeks later for TdTomato and S100β or GFAP. As in the uninjured nerve (Figure 1F), TdTomato-positive cells were not colabeled for S100β or GFAP (Figures 5C and 5D). Thus, *Dermo1*-tagged mesenchymal cells do not apparently differentiate into Schwann cells in either the skin or the nerve, even following injury.

Human SKPs Can Be Generated from Both Facial and Foreskin Dermis, and Those from the Foreskin Express Genes Characteristic of Mesodermally Derived Rodent SKPs

We next asked whether human SKPs of nonneural crest origin could generate Schwann cells. By analogy to other vertebrates, it is thought that human facial dermis is neural crest derived whereas dermis elsewhere is of mesodermal origin. We therefore compared human SKPs made from human facial versus foreskin dermis to provide support for the idea that, like the dermis itself, they were of two different embryonic origins.

For this analysis, SKPs were isolated from neonatal human foreskin as previously described (Toma et al., 2005). We also used the same technique to isolate SKPs from discarded facial tissue of children younger than 2 years old that were undergoing facial reconstruction surgery. Immunostaining of the facial SKPs after one passage showed that they expressed fibronectin, vimentin, and versican (Figures 5E–5G), characteristic SKPs markers. Differentiation of facial SKPs under previously defined neural conditions (Toma et al., 2005; Steinbach et al., 2011) led to the genesis of βIII-tubulin-expressing cells with the morphology of neurons (Figure 5H) and SMA-positive myofibroblasts or smooth muscle cells, as demonstrated by immunostaining (Figure 5I). When facial SKPs were instead plated in Schwann cell conditions, immunostaining identified a small proportion of bipolar cells expressing p75NTR and P0 (Figure 5J). Finally, when facial SKPs were differentiated under osteogenic conditions (Lavoie et al., 2009), we observed small alizarin red-positive nodules indicating osteogenic calcium mineralization (Figure 5K). Thus, human facial SKPs were similar to foreskin SKPs with regard to their differentiation repertoire.

We therefore performed microarrays, comparing four independent samples each of facial and foreskin SKPs on the Affymetrix GeneChip Human Gene 2.0 ST Array (GEO accession number GSE57519). Spearman rank correlation (Figure 6A) showed that foreskin and facial SKPs were highly similar to each other, in spite of the genetic variability inherent to human samples. Unbiased hierarchical clustering using correlation distance and Ward's clustering method (Figure 6B) confirmed this conclusion with high confidence (AU p value and BP values between 88 and 100). Nonetheless, the two groups clustered independently, indicating reproducible differences.

We also performed differential expression analysis using the LIMMA bioconductor package (Smyth, 2004;

(A) Spearman rank correlation matrix computed for the microarray experiments based upon all of the 20,412 probesets, as visualized by color-coding, with red and blue representing the most highly and the least correlated samples, respectively.
(B) Microarray data sets were clustered using unbiased hierarchical clustering with correlation distance and Ward's clustering method. AU and BP values were all between 95 and 100, indicating high confidence.
(C and D) Venn diagrams (C) or bar graphs (D) of pair-wise comparisons between dorsal SKP-SCs versus nerve-SCs and dorsal SKP-SCs versus dorsal SKPs using an analysis similar to one-way ANOVA implemented in the LIMMA bioconductor package for genes that are 2-fold significantly different ($p < 0.05$, BH).
(E) A heatmap of the microarray data for 48 genes expressed in Schwann cells during their differentiation from neural crest precursors to myelinating Schwann cells. Red and green indicate the highest and lowest relative levels of expression, as defined by the color key.
(F) RT-PCR analysis of the Schwann cell mRNAs *Krox20*, *Sox10*, *P0*, and *Oct6* mRNAs in equal amounts of total RNA from rat dorsal SKP-SCs and rat nerve-SCs. Each lane represents an independent isolation. *Gapdh* mRNA was used as a control. −RT refers to the nerve-SC samples analyzed without addition of reverse transcriptase.
(G) RT-PCR analysis of *Hoxa5* and *Hoxc6* mRNAs in equal amounts of total RNA from two to three independent isolates of dorsal versus facial SKPs and dorsal SKP-SCs versus facial SKP-SCs. *Gapdh* mRNA was used as a positive control, and −RT refers to the dorsal trunk SKP samples without reverse transcriptase.

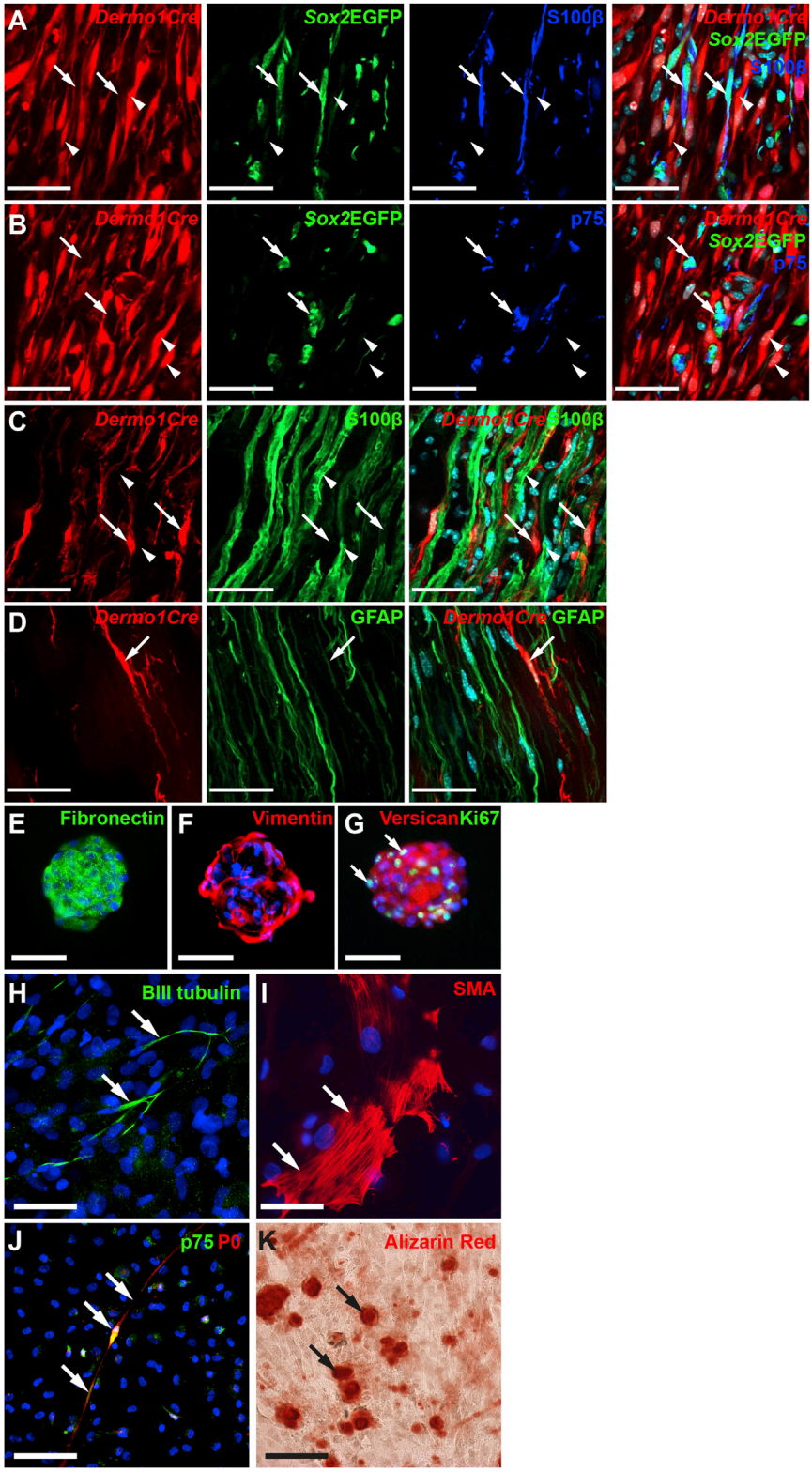

Figure 5. Mesenchymally Derived *Dermo1*-Positive Cells Do Not Generate Schwann Cells following Injury, and Characterization of SKPs Generated from Human Facial Skin

(A and B) Confocal micrographs of sections through the regenerated dorsal dermis of adult *Dermo1*$^{Cre/+}$;*R26TdTomato*$^{fl/+}$; Sox2:EGFP mice 9 days following a punch wound, immunostained for EGFP (A and B, green) to detect the Sox2 reporter and for S100β (A, blue) or p75NTR (B, blue). TdTomato (A and B, red) was visualized without immunostaining. The right panels show the merges. Arrows indicate cells that coexpress Sox2:EGFP and S100β (A) or p75NTR (B), but not the Dermo1Cre reporter. Arrowheads identify cells that are only positive for TdTomato.

(C and D) Confocal micrographs of longitudinal sections through the regenerated sciatic nerve of an adult *Dermo1*$^{Cre/+}$; *R26TdTomato*$^{fl/+}$ mouse 14 days following nerve crush, immunostained for TdTomato (red) and either S100β (C, green) or GFAP (D, green). Arrows indicate cells positive only for the Dermo1Cre reporter, and arrowheads in (C) denote cells positive only for S100β.

(E–G) Secondary-passage human facial SKP spheres immunostained for fibronectin (E, green), vimentin (F, red), or versican (G, red) and the proliferation marker Ki67 (G, green).

(H and I) Human facial SKPs differentiated under neurogenic conditions, immunostained for βIII-tubulin to identify putative neurons (H, green, arrows) or smooth muscle actin (SMA) to detect smooth muscle cells/myofibroblasts (I, red, arrows).

(J) Human facial SKPs differentiated under Schwann cell conditions and immunostained for p75NTR (green) and P0 (red). Arrows denote a double-positive cell with the morphological characteristics of a Schwann cell.

(K) Human facial SKPs differentiated under osteogenic conditions and stained with alizarin red to detect bone mineralization. Arrows denote positive nodules.

SKPs in (E)–(J) were counterstained with Hoechst 33258 (blue). Scale bars represent 25 μm (A–D) and 50 μm (E–K).

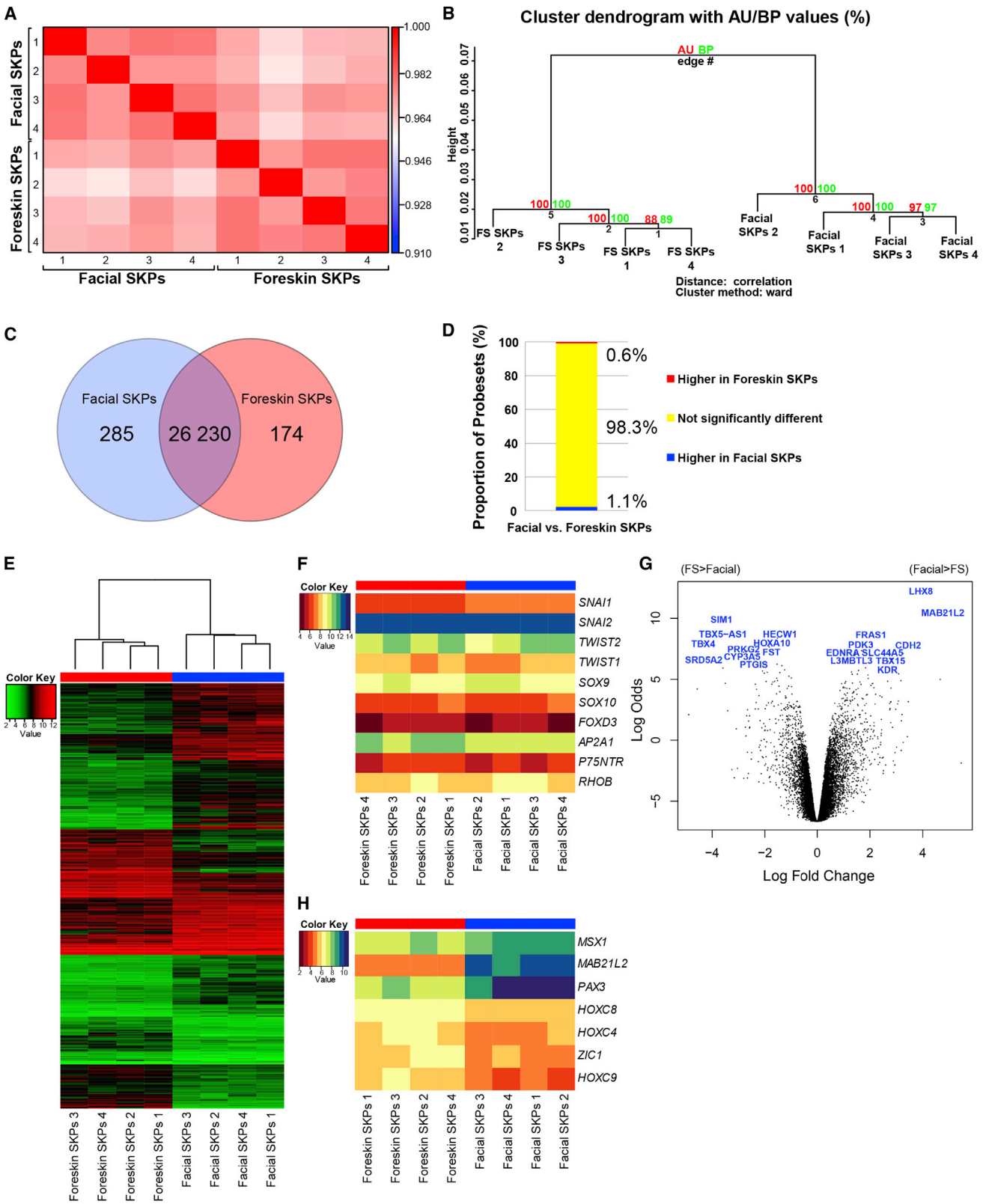

(legend on next page)

Wettenhall and Smyth, 2004). Only 459 genes, or less than 2%, showed significant differences of 2-fold or greater between foreskin versus facial SKPs ($p < 0.05$, BH) (Figures 6C and 6D). The expression levels of these genes are shown as a heatmap (Figure 6E). A more limited heatmap showed that ten genes associated with a neural crest-like phenotype were similarly expressed in the two groups (Figure 6F).

These data indicate that facial and foreskin SKPs were highly similar. Nonetheless, a standard pairwise differential expression comparison using linear models demonstrated that a subset of genes were significantly differentially expressed (Figure 6G; Table S1 available online). We therefore asked whether these two populations differentially expressed genes diagnostic of their different embryonic origins. A heatmap comparison (Figure 6H) of genes previously shown to distinguish facial versus trunk-derived rodent SKPs (Jinno et al., 2010) showed that *MSX1*, *MAB21L2*, and *PAX3*, genes diagnostic of rodent neural crest-derived facial SKPs, were also expressed more highly in human facial SKPs. Conversely, *HOXC9*, *HOXC4*, *HOXC8*, and *ZIC1*, genes diagnostic of rodent mesodermally derived dorsal SKPs, were expressed more highly in human foreskin SKPs (Figure 6H). These data are therefore consistent with the conclusion that human facial versus foreskin SKPs derive from neural crest versus mesodermal origins, as do their rodent counterparts.

Human Foreskin-Derived SKPs Also Generate Functional Schwann Cells

We next asked whether human foreskin SKPs could give rise to functional Schwann cells. When expanded and passaged foreskin SKPs were differentiated under Schwann cell conditions they generated an adherent bed of cells underneath many bipolar, phase-bright cells (Figure 7A). These bipolar cells were immunopositive for p75NTR and S100β and bound the NECL1-Fc (Figures 7A and 7B).

We asked whether these putative human SKP-SCs could myelinate by coculturing them with embryonic rat dorsal root ganglion (DRG) neurons treated with cytosine arabinoside to eliminate endogenous rat Schwann cells. These cocultures were treated with fetal bovine serum and ascorbic acid to induce myelination and immunostained 12 days later for myelin basic protein (MBP) to visualize myelin segments and for the paranodal junction-specific protein CASPR. There was no myelination in cultures containing only DRG neurons (data not shown). In contrast, segments of myelin with paranodal junctions were evident in cultures where human SKP-SCs had been added (Figure 7C). We also immunostained these cocultures with antibodies recognizing just rodent or both rodent and human gliomedin, a node of Ranvier protein (Eshed et al., 2005). As predicted, nodes were positively stained with the antibody that recognized human gliomedin, but not with the rat-specific antibody (Figure 7E). In contrast, in cultures of rat DRG neurons containing endogenous rat Schwann cells that were induced to myelinate, both gliomedin antibodies recognized the nodes (Figure 7D).

Since foreskin SKP-SCs could myelinate in culture, we asked whether they could also do so in vivo. SKP-SCs were isolated from differentiated SKP cultures by magnetic bead sorting after decorating them with the NECL1-Fc (Figure 7F), as previously reported for rodent Schwann cells (Spiegel and Peles, 2009). We injected these purified SKP-SCs into the sciatic nerves of NOD/SCID mice previously treated with lysolecithin to induce local demyelination (Gregson, 1989). Transplanted nerves were then immunostained with a human mitochondria-specific antibody. At 4 days posttransplant, many human cells were present in the transplant region and some were aligned along βIII-tubulin-positive axons (Figure 7G). At 30 days posttransplant, some human mitochondrial antigen-positive cells expressed S100β, a marker for the nonmyelinating Schwann

Figure 6. Human Facial versus Foreskin-Derived SKPs Are Highly Similar at the Transcriptome Level but Differentially Express Genes Indicative of Distinct Origins

Microarray analysis (GEO accession number GSE57519) of four samples each of neonatal human facial SKPs (facial SKPs 1 to 4) and foreskin SKPs (FS or foreskin SKPs 1 to 4).

(A) Spearman rank correlation matrix computed for the microarray experiments based upon all of the 26,689 probesets, as visualized by color-coding, with red and blue representing the most and least highly correlated samples, respectively.

(B) Microarray data sets were clustered using unbiased hierarchical clustering with correlation distance and Ward's clustering method. AU and BP values between 88 and 100 indicate high confidence.

(C and D) Venn diagram (C) or bar graph (D) depicting numbers of genes identified as 2-fold significantly different ($p < 0.05$, BH) using an analysis similar to one-way ANOVA implemented in the LIMMA bioconductor package.

(E) Heatmap of the microarray data for 459 genes that were 2-fold significantly different ($p < 0.05$, BH).

(F) Heatmap of the microarray data for genes associated with a neural crest phenotype.

(G) Volcano plot of a standard pairwise differential expression comparison of facial versus foreskin SKPs. A positive log fold change indicates greater expression in facial SKPs relative to foreskin SKPs.

(H) Heatmap of the microarray data for genes previously shown to differ between rodent neural crest-derived facial SKPs and mesodermally derived dorsal trunk SKPs (Jinno et al., 2010).

See also Table S1.

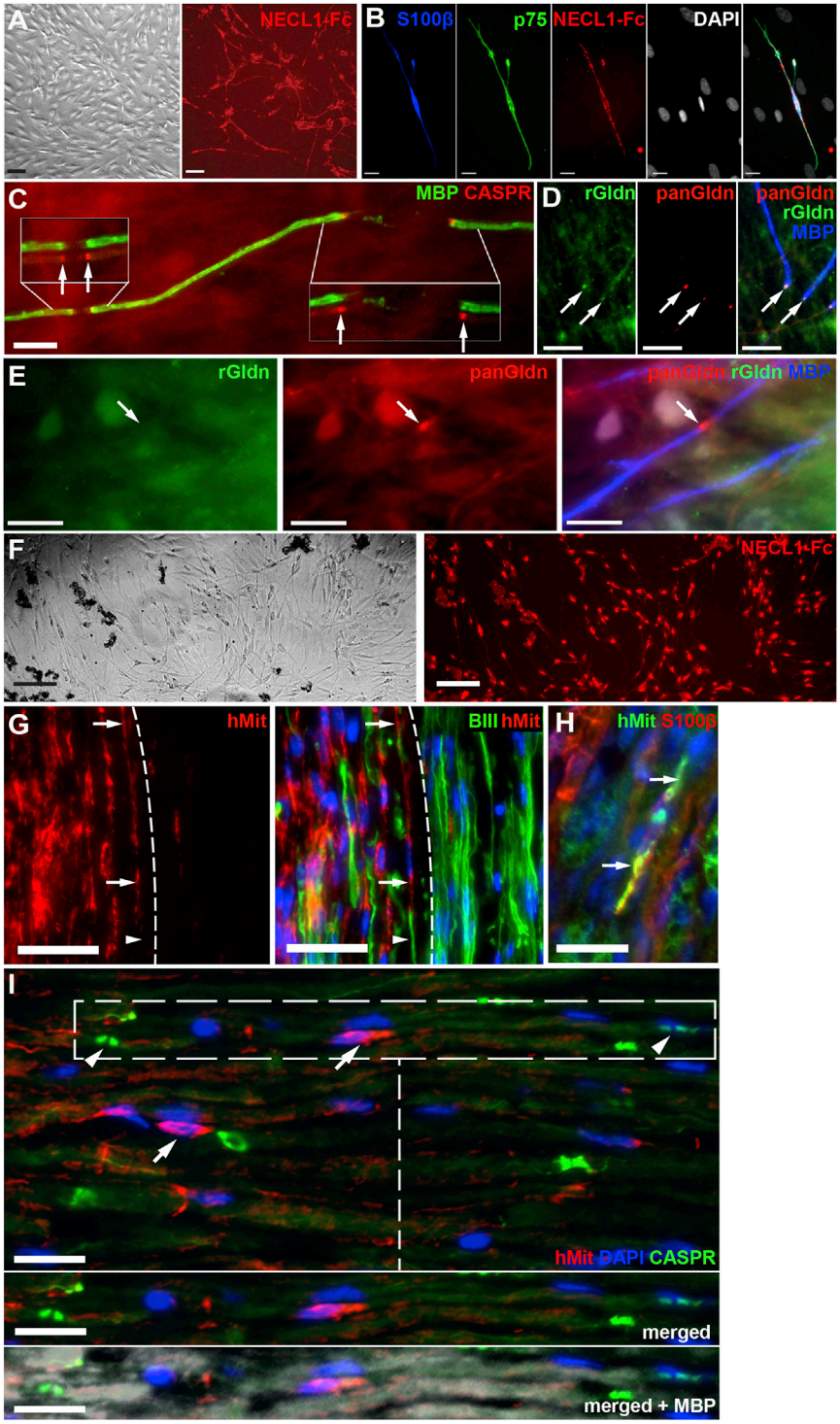

Figure 7. Human Foreskin-Derived SKPs Can Differentiate into Functional, Myelinating Schwann Cells

(A) Bright-field (left) and fluorescence (right) micrographs of living human SKPs differentiated in Schwann cell conditions and decorated with the NECL1-Fc (red).

(B) Micrographs of cultures as in (A) that were decorated with NECL1-Fc (red), fixed and immunostained for S100β (blue) and p75NTR (green).

(C) Human SKP-derived Schwann cells were cocultured with embryonic rat sensory neurons, and myelination was induced for 12 days. Cocultures were immunostained for MBP (green) and the paranodal junction-specific protein CASPR (red, arrows) to visualize myelin segments. The boxed areas show the indicated regions at higher magnification, with the MBP and CASPR signals shown separately. Arrows denote paranodal junctions.

(D and E) Cultures similar to those in (C), where DRG neurons were cocultured with endogenous rat Schwann cells (D) or with human SKP-SCs (E). Cocultures were immunostained for MBP (blue) and with antibodies that recognize either rat gliomedin alone (green; rGldn) or both human and rat gliomedin (red; panGldn). Arrows in (D) denote puncta that are positive with both gliomedin antibodies, while the arrow in (E) denotes a human node that is recognized by the pan-gliomedin, but not by the rat-specific gliomedin, antibody.

(F) Bright-field (left) and fluorescence (right) micrographs of living human SKP-SCs that were decorated with the NECL1-Fc (red) and then sorted using magnetic beads (dark precipitates, left).

(G–I) Micrographs of longitudinal sections through the sciatic nerves of NOD/SCID mice that were demyelinated using lysolethicin and were then transplanted with a sorted, enriched population of human SKP-SCs (as seen in F). Sections were immunostained either 4 days (G) or 1 month (H and I) after transplantation. In (G), sections were immunostained for human mitochondrial antigen to visualize transplanted cells (red) and βIII-tubulin (green) to visualize axons. The right panel shows the merge, and the dashed line demarcates the regions that did and did not receive transplanted cells. Arrows denote human SKP-SCs closely associated with endogenous axons (green, arrowhead). In (H), 1 month following transplantation with human SKP-SCs, longitudinal sections of the transplanted nerve were immunostained for human mitochondrial antigen (green) and the Schwann cell protein S100β (red). Arrows denote a double-positive cell with the morphology of a nonmyelinating Schwann cell. DAPI (blue) was used as nuclear counterstain in (G and H). In (I), sections

(legend continued on next page)

cell phenotype (Figure 7H). Moreover, cell bodies positive for human mitochondrial antigen were aligned along MBP-positive myelin sheaths that were associated with the paranodal protein CASPR (Figure 7I), consistent with a myelinating Schwann cell phenotype. Thus, human foreskin-derived SKPs can generate bona fide Schwann cells that myelinate axons both in culture and in vivo.

DISCUSSION

Data presented here provide strong support for the conclusion that rodent and human mesenchymal precursors of nonneural crest origin can, without genetic manipulation, generate a peripheral neural cell type thought only to derive from the neural crest. A key question then is why a dermal mesenchymal precursor would have this potential. During embryogenesis, neural crest precursors give rise to both mesenchymal and peripheral neural cell types (Le Douarin, 1982). Some of these neural crest precursors persist in the adult and maintain their dual potential. For example, the precursors that generate facial dermis are neural crest derived, persist in the adult, and, when cultured as SKPs, maintain their neural crest potential (Fernandes et al., 2004; Jinno et al., 2010). However, while facial dermis is neural crest derived, the rest of the vertebrate dermis is of mesodermal origin (Christ and Ordahl, 1995; Mauger, 1972), providing a classic example of developmental convergence. Nonetheless, in spite of these different developmental origins, we previously showed that SKPs generated from facial and trunk dermis are highly similar (Jinno et al., 2010), and here we show that even mesodermally derived dorsal SKPs can generate bona fide myelinating Schwann cells. We propose that, while surprising, the peripheral neural differentiation potential of dermal mesenchymal precursors is another example of the developmental convergence of neural crest and mesodermal lineages.

A second key question arising from these findings is whether adult mesenchymal precursors ever generate peripheral neural cells in vivo. Data presented here argue that this is unlikely. In particular, the *Dermo1Cre* mesenchymal reporter gene was not expressed by Schwann cells in normal skin or following injury to the skin or sciatic nerve, consistent with our recent work showing that Schwann cells in regenerating skin were all of neural crest origin (Johnston et al., 2013). Thus, the in vivo environment restricts these dermal mesenchymal precursors so that they do not cross lineage boundaries, much as previously described for the neural crest developmentally (Le Douarin, 1982).

A third question involves directed reprogramming of mouse embryonic fibroblasts or dermal fibroblasts to neural cell types (Abdullah et al., 2012). These findings are interpreted as reflecting genetically driven reprogramming/transdifferentiation, but our data suggest that these manipulations might be unmasking an intrinsic peripheral neural potential in endogenous dermal mesenchymal precursors rather than transdifferentiating cells incapable of making neural cell types.

A fourth question is whether mesenchymal precursors in other tissues can cross the mesodermal/neural crest lineage boundary. In this regard, mesenchymal tissues such as bone and adipose tissue are also developmentally generated by both the neural crest and mesoderm, and bone marrow and adipose-derived mesenchymal precursors have been reported to generate cells with neural properties (for example, see Caddick et al., 2006). However, since neural crest precursors exist in the nerves that innervate virtually all tissues, and since these precursors were not definitively removed from the mesenchymal precursor preparations in most studies, then this remains an open question.

Our findings demonstrate that nonneural crest-derived mesenchymal precursors can differentiate into bona fide peripheral glia in the absence of genetic manipulation. Our study adds to a body of work showing that somatic tissue precursors display greater potential when cultured than they do in vivo. These findings therefore set the stage for asking about the intrinsic nature and flexibility of lineage bias and for defining the cues that restrict precursor cells to ensure that they only generate appropriate progeny in vivo.

EXPERIMENTAL PROCEDURES

Animals

This study was approved by the animal care committee of the Hospital for Sick Children, in accordance with Canadian Council on Animal Care guidelines. *Dermo1*$^{Cre/+}$ (Yu et al., 2003), *R26Td Tomato*$^{fl/+}$ (Madisen et al., 2010), *R26YFP*$^{fl/+}$ (Srinivas et al., 2001), and *Sox2*$^{+/EGFP}$ (Ellis et al., 2004) mice were as described (Johnston et al., 2013). Sprague-Dawley rats, either wild-type (Charles River) or GFP expressing (SLC, Japan), were purchased and maintained as described (Biernaskie et al., 2009). NOD/SCID mice were obtained from Jackson Laboratory. Animal care after surgery was as described in the Supplemental Experimental Procedures.

were immunostained for human mitochondrial antigen (red, arrows), MBP to show myelin segments (white), and CASPR to show nodes of Ranvier (green, arrowhead). The top two panels show the merge of signals for human mitochondrial antigen and CASPR and the bottom panel the merge of all three signals. The boxed area in the top panel is shown at higher magnification in the bottom two panels.
Scale bars represent 100 μm (A and F), 30 μm (B), 10 μm (C–E), 50 μm (G), and 20 μm (H and I).

Primary Cultures and Differentiation

Rodent SKPs were cultured and passaged as previously described (Toma et al., 2001; Biernaskie et al., 2009; Fernandes et al., 2004) and detailed in the Supplemental Experimental Procedures. For human SKPs (Toma et al., 2005), anonymized foreskin tissue from voluntary circumcisions or facial tissue from facial reconstruction surgeries of young children were obtained with approval of the research ethics board of the Hospital for Sick Children.

Differentiation of rodent and human Schwann cells was performed as described (Biernaskie et al., 2006; McKenzie et al., 2006) (Supplemental Experimental Procedures). Differentiation of human SKPs was performed as described (Lavoie et al., 2009; Toma et al., 2005) (Supplemental Experimental Procedures). Schwann cells were isolated from the sciatic nerves of 1.5- to 2-month-old Sprague-Dawley rats as detailed in the Supplemental Experimental Procedures. Compartmented cultures of neonatal rat sympathetic neurons were prepared as previously described (Singh and Miller, 2005). Seven days after cultures were established, SKP-SCs were plated in side compartments as detailed in the Supplemental Experimental Procedures. For myelination assays, dissociated embryonic day 15 DRG neurons were prepared as described (Eshed et al., 2005), and human SKPs differentiated under Schwann cell conditions were added for 4 days and switched to myelination conditions for an additional 12 days (Supplemental Experimental Procedures).

Cell Sorting

Dorsal skin from *Dermo1*$^{Cre/+}$;*R26YFP*$^{fl/+}$ mice was dissociated to single cells and sorted for YFP on a MoFlo (Dako) with viable cells identified by propidium iodide exclusion. YFP-positive and negative fractions were collected and resuspended in SKPs growth media for 10 days to quantify sphere growth. Alternatively, primary-passage SKP spheres from *Dermo1*$^{Cre/+}$;*R26YFP*$^{fl/+}$ or *Dermo1*$^{Cre/+}$;*R26TdTomato*$^{fl/+}$ mice were dissociated to single cells and sorted for YFP or TdTomato. In all flow cytometry experiments, wild-type littermates were used to determine negative levels for setting gates. Magnetic sorting of human SKP-SCs was based on Spiegel and Peles (2009), where NECL4 was bound by soluble recombinant, fluorescently prelabeled Necl1-human Fc (Necl1-Fc), as modified for magnetic bead sorting (described in the Supplemental Experimental Procedures).

In Vivo Injury and Transplantation Experiments

Young-adult NOD/SCID mice were used for transplant experiments. For mouse cell experiments, the sciatic nerve was crushed and 2×10^5 cells were injected distal to the crush site. For human cell experiments, myelin was locally ablated in the sciatic nerve by injection of 1% lysolecithin (Avanti Polar Lipids) in Locks solution (Gregson, 1989) and 2×10^5 cells were injected 6 days later as described (McKenzie et al., 2006). Additional details are in the Supplemental Experimental Procedures. For adult skin experiments, 6 mm full-thickness punch wounds were administered to the dorsal trunk as described (Johnston et al., 2013).

Immunostaining and Microscopy

Immunostaining of cells and tissue sections was performed as previously described (Biernaskie et al., 2009; Johnston et al., 2013). Antibodies and details of microscopy are in the Supplemental Experimental Procedures.

Microarrays and Statistical Analyses

RNA was isolated from three biological replicates of passage 2 adult rat nerve-derived and SKP-derived Schwann cells and from four different replicates each for human facial versus foreskin SKPs using TRIzol reagent (Invitrogen) and purified with the RNeasy Mini Kit (QIAGEN). RNA was converted into cDNA by reverse transcription with the Ambion Whole Transcript (WT) Expression Kit (Applied Biosystems). cDNA was hybridized to the GeneChip Rat Gene 1.0 Sense Target ST Array or the GeneChip Human Gene 2.0 Sense Target ST Array (Affymetrix) using the GeneChip Fluidics Station 450 (Affymetrix). The hybridized microarray image was scanned with the GeneChip Scanner 3000 7G (Affymetrix). Raw probe intensity values were background corrected, normalized with quantile normalization, transformed into the $\log_2$ scale, and summarized into probesets using the Robust Multichip Analysis (RMA) algorithm at the gene level in the Affymetrix Expression Console program. To reduce the false-discovery rate, only probesets for annotated genes were used for the LIMMA bioconductor package in R. Bayesian statistics were calculated using the eBayes function and the Benjamini-Hochberg (BH) procedure was used to correct for multiple testing errors. Those genes with BH-corrected p value < 0.05 were considered statistically significant. Spearman rank correlation was generated in Affymetrix Expression Console. Unbiased hierarchical clustering was performed in R with the pvclust package using correlation distance and Ward's clustering method. Heatmaps were generated using the gplots package in R.

RT-PCR for Selected Genes

RNA was isolated from rat nerve SCs, dorsal SKP-SCs, facial SKP-SCs, dorsal SKPs, and facial SKPs using TRIzol reagent and purified with the Ambion RiboPure kit (Invitrogen). Reverse transcription was performed using the RevertAid H Minus First Strand cDNA Synthesis kit (K1632, Thermo Scientific). Primers are listed in the Supplemental Experimental Procedures.

ACCESSION NUMBERS

The GEO accession number for the rat and human microarray data reported in this paper is GSE57519.

SUPPLEMENTAL INFORMATION

Supplemental Information includes Supplemental Experimental Procedures and one table and can be found with this article online at http://dx.doi.org/10.1016/j.stemcr.2014.05.011.

ACKNOWLEDGMENTS

This work was funded by CIHR grant MOP-64211 and a Canadian SCN Global Research grant to F.D.M. K.F., M.P.K., A.P.W.J., and S.D. are funded by scholarships from the Jacobs Ladder Foundation, CIHR, the Ontario Stem Cell Initiative, and the CIHR Training Program in Regenerative Medicine, respectively. F.D.M. and D.R.K. hold Canada Research Chairs, and F.D.M. is an HHMI Senior

International Research Scholar. We thank Benigno Aquino and Vania Ariosa for technical advice and assistance.

Received: October 17, 2013
Revised: May 14, 2014
Accepted: May 15, 2014
Published: June 19, 2014

REFERENCES

Abdullah, A.I., Pollock, A., and Sun, T. (2012). The path from skin to brain: generation of functional neurons from fibroblasts. Mol. Neurobiol. *45*, 586–595.

Biernaskie, J.A., McKenzie, I.A., Toma, J.G., and Miller, F.D. (2006). Isolation of skin-derived precursors (SKPs) and differentiation and enrichment of their Schwann cell progeny. Nat. Protoc. *1*, 2803–2812.

Biernaskie, J., Sparling, J.S., Liu, J., Shannon, C.P., Plemel, J.R., Xie, Y., Miller, F.D., and Tetzlaff, W. (2007). Skin-derived precursors generate myelinating Schwann cells that promote remyelination and functional recovery after contusion spinal cord injury. J. Neurosci. *27*, 9545–9559.

Biernaskie, J., Paris, M., Morozova, O., Fagan, B.M., Marra, M., Pevny, L., and Miller, F.D. (2009). SKPs derive from hair follicle precursors and exhibit properties of adult dermal stem cells. Cell Stem Cell *5*, 610–623.

Caddick, J., Kingham, P.J., Gardiner, N.J., Wiberg, M., and Terenghi, G. (2006). Phenotypic and functional characteristics of mesenchymal stem cells differentiated along a Schwann cell lineage. Glia *54*, 840–849.

Christ, B., and Ordahl, C.P. (1995). Early stages of chick somite development. Anat. Embryol. (Berl.) *191*, 381–396.

Ellis, P., Fagan, B.M., Magness, S.T., Hutton, S., Taranova, O., Hayashi, S., McMahon, A., Rao, M., and Pevny, L. (2004). SOX2, a persistent marker for multipotential neural stem cells derived from embryonic stem cells, the embryo or the adult. Dev. Neurosci. *26*, 148–165.

Eshed, Y., Feinberg, K., Poliak, S., Sabanay, H., Sarig-Nadir, O., Spiegel, I., Bermingham, J.R., Jr., and Peles, E. (2005). Gliomedin mediates Schwann cell-axon interaction and the molecular assembly of the nodes of Ranvier. Neuron *47*, 215–229.

Fernandes, K.J.L., McKenzie, I.A., Mill, P., Smith, K.M., Akhavan, M., Barnabé-Heider, F., Biernaskie, J., Junek, A., Kobayashi, N.R., Toma, J.G., et al. (2004). A dermal niche for multipotent adult skin-derived precursor cells. Nat. Cell Biol. *6*, 1082–1093.

Gregson, N.A. (1989). Lysolipids and membrane damage: lysolecithin and its interaction with myelin. Biochem. Soc. Trans. *17*, 280–283.

Hunt, D.P.J., Morris, P.N., Sterling, J., Anderson, J.A., Joannides, A., Jahoda, C., Compston, A., and Chandran, S. (2008). A highly enriched niche of precursor cells with neuronal and glial potential within the hair follicle dermal papilla of adult skin. Stem Cells *26*, 163–172.

Jessen, K.R., and Mirsky, R. (2005). The origin and development of glial cells in peripheral nerves. Nat. Rev. Neurosci. *6*, 671–682.

Jinno, H., Morozova, O., Jones, K.L., Biernaskie, J.A., Paris, M., Hosokawa, R., Rudnicki, M.A., Chai, Y., Rossi, F., Marra, M.A., and Miller, F.D. (2010). Convergent genesis of an adult neural crest-like dermal stem cell from distinct developmental origins. Stem Cells *28*, 2027–2040.

Johnston, A.P.W., Naska, S., Jones, K., Jinno, H., Kaplan, D.R., and Miller, F.D. (2013). Sox2-mediated regulation of adult neural crest precursors and skin repair. Stem Cell Reports *1*, 38–45.

Lavoie, J.-F., Biernaskie, J.A., Chen, Y., Bagli, D., Alman, B., Kaplan, D.R., and Miller, F.D. (2009). Skin-derived precursors differentiate into skeletogenic cell types and contribute to bone repair. Stem Cells Dev. *18*, 893–906.

Le Douarin, N. (1982). The Neural Crest (Cambridge: Cambridge University Press).

Li, L., Cserjesi, P., and Olson, E.N. (1995). Dermo-1: a novel twist-related bHLH protein expressed in the developing dermis. Dev. Biol. *172*, 280–292.

Madisen, L., Zwingman, T.A., Sunkin, S.M., Oh, S.W., Zariwala, H.A., Gu, H., Ng, L.L., Palmiter, R.D., Hawrylycz, M.J., Jones, A.R., et al. (2010). A robust and high-throughput Cre reporting and characterization system for the whole mouse brain. Nat. Neurosci. *13*, 133–140.

Mauger, A. (1972). [The role of somitic mesoderm in the development of dorsal plumage in chick embryos. II. Regionalization of the plumage-forming mesoderm]. J. Embryol. Exp. Morphol. *28*, 343–366.

Maurel, P., Einheber, S., Galinska, J., Thaker, P., Lam, I., Rubin, M.B., Scherer, S.S., Murakami, Y., Gutmann, D.H., and Salzer, J.L. (2007). Nectin-like proteins mediate axon Schwann cell interactions along the internode and are essential for myelination. J. Cell Biol. *178*, 861–874.

McKenzie, I.A., Biernaskie, J., Toma, J.G., Midha, R., and Miller, F.D. (2006). Skin-derived precursors generate myelinating Schwann cells for the injured and dysmyelinated nervous system. J. Neurosci. *26*, 6651–6660.

Singh, K.K., and Miller, F.D. (2005). Activity regulates positive and negative neurotrophin-derived signals to determine axon competition. Neuron *45*, 837–845.

Smyth, G.K. (2004). Linear models and empirical bayes methods for assessing differential expression in microarray experiments. Stat. Appl. Genet. Mol. Biol. *3*, Article3.

Spiegel, I., and Peles, E. (2009). A novel method for isolating Schwann cells using the extracellular domain of Necl1. J. Neurosci. Res. *87*, 3288–3296.

Srinivas, S., Watanabe, T., Lin, C.S., William, C.M., Tanabe, Y., Jessell, T.M., and Costantini, F. (2001). Cre reporter strains produced by targeted insertion of EYFP and ECFP into the ROSA26 locus. BMC Dev. Biol. *1*, 4.

Steinbach, S.K., El-Mounayri, O., DaCosta, R.S., Frontini, M.J., Nong, Z., Maeda, A., Pickering, J.G., Miller, F.D., and Husain, M. (2011). Directed differentiation of skin-derived precursors into functional vascular smooth muscle cells. Arterioscler. Thromb. Vasc. Biol. *31*, 2938–2948.

Toma, J.G., Akhavan, M., Fernandes, K.J., Barnabé-Heider, F., Sadikot, A., Kaplan, D.R., and Miller, F.D. (2001). Isolation of multipotent adult stem cells from the dermis of mammalian skin. Nat. Cell Biol. *3*, 778–784.

Toma, J.G., McKenzie, I.A., Bagli, D., and Miller, F.D. (2005). Isolation and characterization of multipotent skin-derived precursors from human skin. Stem Cells *23*, 727–737.

Wettenhall, J.M., and Smyth, G.K. (2004). limmaGUI: a graphical user interface for linear modeling of microarray data. Bioinformatics *20*, 3705–3706.

Wong, C.E., Paratore, C., Dours-Zimmermann, M.T., Rochat, A., Pietri, T., Suter, U., Zimmermann, D.R., Dufour, S., Thiery, J.P., Meijer, D., et al. (2006). Neural crest-derived cells with stem cell features can be traced back to multiple lineages in the adult skin. J. Cell Biol. *175*, 1005–1015.

Yu, K., Xu, J., Liu, Z., Sosic, D., Shao, J., Olson, E.N., Towler, D.A., and Ornitz, D.M. (2003). Conditional inactivation of FGF receptor 2 reveals an essential role for FGF signaling in the regulation of osteoblast function and bone growth. Development *130*, 3063–3074.